Supracolloidal Reaction Kinetics of Janus Spheres

Qian Chen,[1] Jonathan K. Whitmer,[1,2] Shan Jiang,[1] Sung Chul Bae,[1]
Erik Luijten,[3, 4] Steve Granick[1,2,5]
[1]Departments of Materials Science and Engineering, [2]Physics, and [5]Chemistry
University of Illinois, Urbana, IL 61801, USA
[3]Department of Materials Science and Engineering and [4]Department of Engineering Sciences and Applied Mathematics, Northwestern University, Evanston, IL 60208, USA

Abstract

Clusters in the form of aggregates of a small number of elemental units display structural, thermodynamic, and dynamic properties different from bulk materials. Here we study the kinetic pathways of self-assembly of "Janus spheres" with hemispherical hydrophobic attraction and show key differences from those characteristic of molecular amphiphiles. Experimental visualization combined with theory and molecular dynamics simulation shows that small, kinetically favored isomers fuse, before they equilibrate, into fibrilar triple helices with at most six nearest neighbors per particle. The time scales of colloidal rearrangement combined with the directional interactions resulting from Janus geometry make this a prototypical system to elucidate, on a mechanistic level and with single-particle kinetic resolution, how chemical anisotropy and reaction kinetics coordinate to generate highly ordered structures.

Clusters, an intermediate level of matter between building block (atom, molecule, or particle) and bulk phase, are found ubiquitously in nature and technology, for example in the nucleation of bulk phases (*1*), nanoparticles (*2*), and protein aggregates in biology (*3*, *4*). While structures that result from isotropic interactions between building blocks are well understood (*5*–*8*), it is more challenging to understand clusters formed from the common case of directional noncovalent interactions (*9*–*17*). On this question, we note that for molecular amphiphiles, such as surfactants, phospholipids, and many block copolymers, the segregation of their polar and nonpolar portions is a major mechanism steering the spontaneous formation of microstructured mesophases with fascinating and useful structures (*9*–*11*). Similarly, colloidal particles, larger than molecules but small enough to sustain Brownian motion, also assemble into clusters owing to directional noncovalent interactions (*12*–*17*). A largely unsolved problem is the question of commonality between these fields. Therefore, combining amphiphilicity with colloidal rigidity, we study "Janus spheres" that are hydrophobic on one hemisphere, negatively charged on the other. An earlier publication from this laboratory described some structures that these hybrid materials form (*18*). Here we address the kinetics of self-assembly at the single-particle level, showing that small, kinetically favored isomers join to form highly ordered but nonequilibrium large-scale structures.

A critical design rule is that the range of interparticle interactions (hydrophobic attraction and electrostatic repulsion) be short relative to particle size and that the interactions be reversible. Clustering then favors densely packed structures with at most six nearest neighbors per particle—in contrast to the more open and less ordered structures formed by particles whose interaction range is larger (*13*). At very low salt concentration particles repel one another electrostatically, whereas at high salt concentrations van der Waals forces cause the particles to aggregate irreversibly (*19*). Therefore, we consider intermediate concentrations of monovalent salt at which amphiphilic clusters self-assemble (*20*).

If the hydrophobic patch is too small, assembly admits clusters composed of at most four particles. However, increase in patch size allows such clusters to grow into larger assemblies, with two constraints: First, particles must approach closely enough to experience hydrophobic attraction; second, the number of nearest neighbors must not exceed six. For Janus particles whose hydrophobic domains are hemispheres, Fig. 1 (panel A) displays pathways of reversible self-assembly, all of which we observe. They form a complex network in which multiple cluster possibilities emanate from every point and, likewise, routes from every point can meet. The hydrophobic patches lend significant orientational freedom to individual particles within the clusters. This promotes dynamical interconversion between clusters through three major mechanisms: step-by-step addition of individual particles, fusion of smaller clusters into a larger

one, and isomerization. The clusters in this regime, with a size range N=2–7, are similar to those formed in depletion-induced assembly of homogeneous particles (*5*), except that for homogeneous particles the clusters must be kept isolated to avoid further aggregation (Fig. S1). Here, cluster aggregation is prevented by electrostatic repulsion between the charged surface regions, allowing clusters to live in close proximity without fusing.

The ability to control the long-range repulsion makes it possible to switch on clustering at will by adding salt to Janus spheres in deionized water. We find that after the distribution of cluster sizes equilibrates (Fig. S2) their shapes continue to change. For example, the capped trigonal bipyramid (CTBP) shape with cluster size N=6 forms first, then gradually isomerizes to the more symmetric octahedral (OCT) shape (Fig. 1, panel B). This kinetic data is consistent with a reversible first-order reaction with rate constants given in the figure caption. In this system, OCT is more stable. Nevertheless the CTBP isomer forms first, since growth proceeds via rotation of a particle in a feeder cluster. Particles located at the cluster ends have the largest rotational freedom and thus act as the points where additional particles join the cluster, causing elongated structures to form. In a cluster, particles constantly jiggle about their mean positions; a process that has analogies to highly excited vibrational motion in molecules, where the vibrations occasionally cause collective rearrangements. Molecular reaction dynamics occur on picosecond or faster time scales *(21)* whereas these colloidal transformations occur on the time

scale of seconds and can be visualized one by one without ensemble averaging. These reaction dynamics are illustrated in Movie S1, showing cluster growth from smaller clusters, and Movies S2 and S3, showing cluster isomerization via different pathways. Unlike micelles formed from molecules, whose predominant growth mechanism is through addition of monomers to pre-existing micelles (*10*), the rigid, spherical shape of these colloidal building blocks allows them to rotate without change of position such that clusters grow at their ends by fusing with other clusters. A second difference is that, unlike molecular micelles whose fluidity encourages shape to equilibrate rapidly, these colloidal clusters possess definite configurations. For the same number of particles in a cluster, there are distinctly different, long-lived shapes.

A minor increase of the salt concentration to 5 mM reduces the electrostatic repulsion to permit the growth of striking helical structures (Fig. 2). Closer inspection shows these to be Boerdijk–Coxeter (BC) helices (*22*), sometimes called Bernal spirals. The formation and stability of helices per se is a consequence of the directionality of the pairwise interactions, which allows them to persist up to the highest particle concentrations (60% after sedimentation), unlike homogeneous particles, which at lower particle concentration form BC helices that become unstable when the concentration is higher (*6*, *7*).

All dense packings of spheres on a cylindrical surface have the same internal energy, since each sphere except those at the ends of the chain interacts with six nearest neighbors (*4*).

This remains true for Janus spheres, provided that each hydrophobic side faces the corresponding hemispheres of all neighbors—a constraint that is satisfied in the very structures that arise from the anisotropic interaction. This is analogous to carbon nanotubes, whose variety of rolled structures result from the same threefold coordinated graphene sheet (*23*). Thus, the absence of helical structures other than the BC helix indicates that either entropic or kinetic effects matter here.

To clarify the relative stability of a range of helical structures (*4*), we calculate their relative free energy as a function of Janus balance, taking into account the rotational entropy of individual Janus particles as well as vibrational modes; a related free-energy landscape is known for spheres with isotropic interactions (*5*). As plotted in Fig. 3A, the 3(0,1,1) helix is in fact thermodynamically favored over the BC helix by a modest amount; here we use the notation proposed when this structure was identified (*4*). Strict quantitative correspondence to the experimental situation is not expected, as a full calculation including collective excitations and chain bending would be formidable to execute, but we can safely conclude that thermodynamically the BC helix is not strongly favored over the 3(0,1,1) helix (other tubular forms have a higher free energy).

Instead, we believe that the BC helices are the observed structure up to the highest particle concentrations because they are selected by kinetics. The preferred initial formation of

capped trigonal bipyramidal N=6 isomers, the basic building block of the BC helix, rather than octahedral N=6 clusters, the basic unit of the 3(0,1,1) helix, causes the former helices to form first. Subsequent transformation relaxation of a BC helix into a 3(0,1,1) helix would require a massive collective change where, in the long-chain limit, one bond must be broken for every group of three spheres. This metastability explains why 3(0,1,1) helices are never observed in the experiment. We confirm the preferred formation of polytetrahedral over polyoctahedral clusters in molecular dynamics (MD) simulations, in particular at high attraction strengths where configurations tend to get trapped. Two further experimental observations strengthen this scenario. Although stable against relaxation into a 3(0,1,1) helix, the BC helices occasionally display a spontaneous switch of handedness (Movies S4 and S5). This is energetically slightly less costly, since only one bond needs to be broken for every four particles. More important, the possible pathway for chirality switching is simpler. Both chirality switching and relaxation to the 3(0,1,1) helix require unfavorable intermediate structures in which one particle has seven nearest neighbors. For the chirality switch, this pivotal particle has four bonds with reduced stability owing to large bond angles. If any of these bonds is broken, the chirality switching either proceeds or the chain returns to its original chirality. For the change from BC to 3(0,1,1), there are three bonds of reduced stability and breaking any of these interrupts the transition; instead, it is one of the stable bonds that needs to be broken for the change to proceed, which is

comparatively harder (see illustrations in Fig. S3). Lastly, in both experiments (Fig. 3B) and MD simulations (Fig. 3C) we observe defects in which an N=7 cluster is incorporated into a helix, reconfirming the kinetically arrested state of these structures, even though individual constituent spheres display considerable mobility. As expected for reversible self-assembly, these fibrilar clusters reform (heal) spontaneously after being torn apart by strong shear. They also fuse with one another through Brownian motion (Movie S6) because the ends, which are most free to rotate, are more reactive than the middle.

The significance of this study is to call attention to the importance of kinetic selection when colloidal amphiphiles cluster. Unlike the rapid shape equilibration of molecular amphiphiles, Janus spheres present transient isomeric structures whose lifetime is so long that before isomers equilibrate they fuse to form the stable, highly ordered nonequilibrium helices described here. Their generalization to colloidal blocks of asymmetric shape (rods, ellipsoids, chains,…) presents an agenda for future work. This work on a prototypical system offers a direction in which to look for the design of new reconfigurable materials from the interplay between equilibration time scale and packing allowed by orientation-specific attraction.

References

1. A. Cacciuto, S. Auer, D. Frenkel, Onset of heterogeneous crystal nucleation in colloidal suspensions. *Nature* **428**, 404–406 (2004).

2. B. Yoon *et al.*, Size-dependent structural evolution and chemical reactivity of gold clusters. *ChemPhysChem.* **8**, 157–161 (2007).

3. T. P. Knowles, A. W. Fitzpatrick, S. Meehan, H. R. Mott, M. Vendruscolo, C. M. Dobson, M. E. Welland, Role of intermolecular forces in defining material properties of protein nanofibrils. *Science* **318**, 1900–1903 (2007).

4. R. O. Erickson, Tubular packings of spheres in biological fine structure, *Science* **181**, 705–716 (1973).

5. G. Meng, N. Arkus, M. P. Brenner, V. N. Manoharan, The free-energy landscape of clusters of attractive hard spheres. *Science* **327**, 560–563 (2010).

6. A. I. Campbell, V. J. Anderson, J. S. van Duijneveldt, P. Bartlett, Dynamical arrest in attractive colloids: the effect of long-range repulsion. *Phys. Rev. Lett.* **94**, 208301 (2005).

7. F. Sciortino, P. Tartaglia, E. Zaccarelli, One-dimensional cluster growth and branching gels in colloidal systems with short-range depletion attraction and screened electrostatic repulsion. *J. Phys. Chem. B* **109**, 21942–21953 (2005).

8. J. Groenewold, W. K. Kegel, Anomalously large equilibrium clusters of colloids. *J. Phys. Chem. B* **105**, 11702–11709 (2001).

9. S. A. Safran, *Statistical Thermodynamics of Surfaces, Interfaces, and Membranes* (Addison Wesley, Reading MA, 1994).

10. I. A. Nyrkova, A. N. Semenov, On the theory of micellization kinetics, *Macromol. Theory Simul.* **14**, 569–585 (2005).

11. S. Jain, F. S. Bates, On the origins of morphological complexity in block copolymer surfactants, *Science* **300**, 460– 464 (2003).

12. S. C. Glotzer, M. J. Solomon, Anisotropy of building blocks and their assembly into complex structures. *Nat. Mater.* **6**, 557–562 (2007).

13. F. Sciortino, A. Giacometti, G. Pastore, Phase diagram of Janus particles. *Phys. Rev. Lett.* **103**, 237801 (2009).

14. W. L. Miller, A. Cacciuto, Hierarchical self-assembly of asymmetric amphiphatic spherical colloidal particles. *Phys. Rev. E* **80**, 021404 (2009).

15. S. Whitelam, S. A. F. Bon, Self-assembly of amphiphilic peanut-shaped nanoparticles. *J. Chem. Phys.* **132**, 074901 (2010).

16. K. Liu, Z. Nie, N. Zhao, W. Li, M. Rubinstein, E. Kumacheva, Step-growth polymerization of inorganic nanoparticles. *Science* **329**,197–200 (2010).

17. Z. Mao, H. Xu, D. Wang, Molecular mimetic self-assembly of colloidal particles. *Adv. Funct. Mater.* **20**, 1053–1074 (2010).

18. L. Hong, A. Cacciuto, E. Luijten, S. Granick, Clusters of amphiphilic colloidal spheres. *Langmuir* **24**, 621–625 (2008).

19. J. W. Goodwin, *Colloids and Interfaces with Surfactants and Polymers. 2nd edn*. (Wiley, Chichester, U.K., 2009), pp.163–181.

20. Materials and methods are available as supporting material on *Science* Online.

21. J. Mikosch *et al.*, Imaging nucleophilic substitution dynamics. *Science* **319**, 183–186 (2008).

22. A. H. Boerdijk, Some remarks concerning close-packing of equal spheres. *Philips Res. Rep.* **7**, 303–313 (1952).

23. H. Dai, Carbon nanotubes: opportunities and challenges. *Surface Science* **500**, 218–241 (2002).

24. We thank Jing Yan for discussions. This work was supported by the DOE (SG, QC, SJ, SCB) and by the NSF (EL and JKW): the U.S. Department of Energy, Division of Materials Science, under Award No. DE-FG02-07ER46471 through the Frederick Seitz Materials Research Laboratory at the University of Illinois at Urbana-Champaign (SG), and the National Science Foundation under Grants DMR-0346914 and DMR-1006430

(EL).

Supporting Online Material

www.sciencemag.org

Materials and Methods

Movie S1, S2, S3, S4, S5, S6

Figure captions

Fig. 1. Clusters formed from Janus spheres with one hydrophobic hemisphere. **Panel A**: Network of reaction pathways, all of which we have observed in experiments at 3.8 mM NaCl. Reaction mechanisms of monomer addition, cluster fusion, and isomerization are denoted by black, red, and blue arrows, respectively. Isomers with N=6 and N=7 elemental spheres are highlighted in boxes. Movie S1 shows a simple example of cluster growth by the fusion of two clusters. **Panel B**: A study of isomerization between two types of N=6 clusters, the capped trigonal bipyramid (CTBP) and the octahedron (OCT). After initiating the cluster process by setting the NaCl concentration at 3.8 mM, the partition of Janus spheres between clusters of different size equilibrates after 20 min (see Fig. S2) but isomerization continues. Once the total number of hexamers (black filled circles) has stabilized, isomerization (fraction of CTBP, blue open circles) is consistent with first-order reaction kinetics in time t, $\mathrm{d[OCT]}/\mathrm{d}t = k_1[\mathrm{CTBP}] - k_{-1}[\mathrm{OCT}]$, time constant 34 minutes, $k_1/k_{-1} = 2.2$, and $k_1 = 0.02\ \mathrm{min}^{-1}$. Here the calculation is based upon the ensemble behavior of many clusters among which individual ones can follow different reaction pathways. Movies S2 and S3 compare different pathways of isomerization.

Fig. 2. Triple helices formed at higher salt concentration and higher particle concentration. **Panel A**: Geometrical representation of helix growth by face-sharing tetrahedra. **Panel B**: Comparison of a small chiral cluster (3.8 mM NaCl) and a longer helical cluster (5 mM NaCl). For both cases, fluorescence images of both right-handed and left-handed structures are shown. **Panel C**: Fluorescence image illustrating the stability of wormlike structures at high volume fraction. Movie S6 shows the fusion of two chiral chains by Brownian motion.

Fig. 3. Consideration of alternative tubular packings and defective structures. **Panel A**: Free energy per particle as a function of Janus balance α, half the opening angle of the hydrophobic patch. These tubular structures (*4*) are the 3(0,1,1) structure whose building block is the octahedral N=6 isomer (red squares); the BC helix whose building block is the capped trigonal bipyramidal N=6 isomer (blue triangles); also, for completeness, the 4(0,1,1) (circles), the (1,3,4) (inverted triangles), and the 2(1,1,2) (diamonds) structures, which have a higher free energy at the experimental Janus balance ($\alpha = 90°$). Including vibrational entropy (*5*), the free-energy difference between the 3(0,1,1) and the BC helix is reduced by 0.19 $k_B T$ per particle for a representative chain length (N=24). At $\alpha = 90°$ this reduces the total free-energy difference by a factor of two. The insets show schematic structures of the 3(0,1,1) and the BC helix. **Panel B**: Example of a kinked chain observed in experiments, in which an N=7 cluster structure

intercalates the predominant BC helix. **Panel C**: Similar structure, now with several intercalating N=7 clusters, observed in molecular dynamics simulation. Particles are colored from white to blue depending on the number of tetrahedra in which they participate, N_{tetra}.

Fig. 1

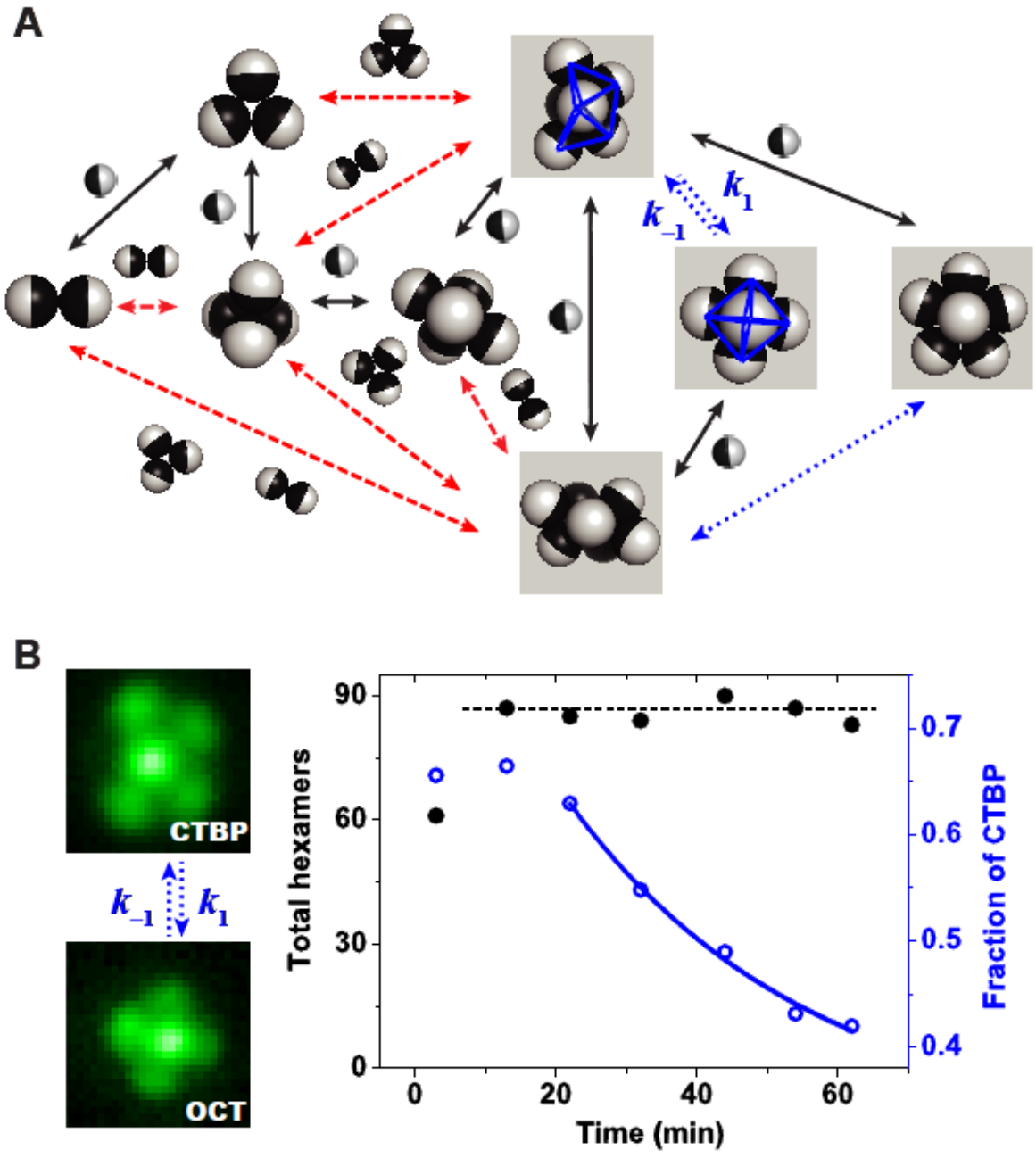
A
k_1
k_{-1}
B
CTBP
OCT
k_{-1}
k_1
Total hexamers
Fraction of CTBP
Time (min)
0
30
60
90
0.4
0.5
0.6
0.7
0
20
40
60

Fig. 2

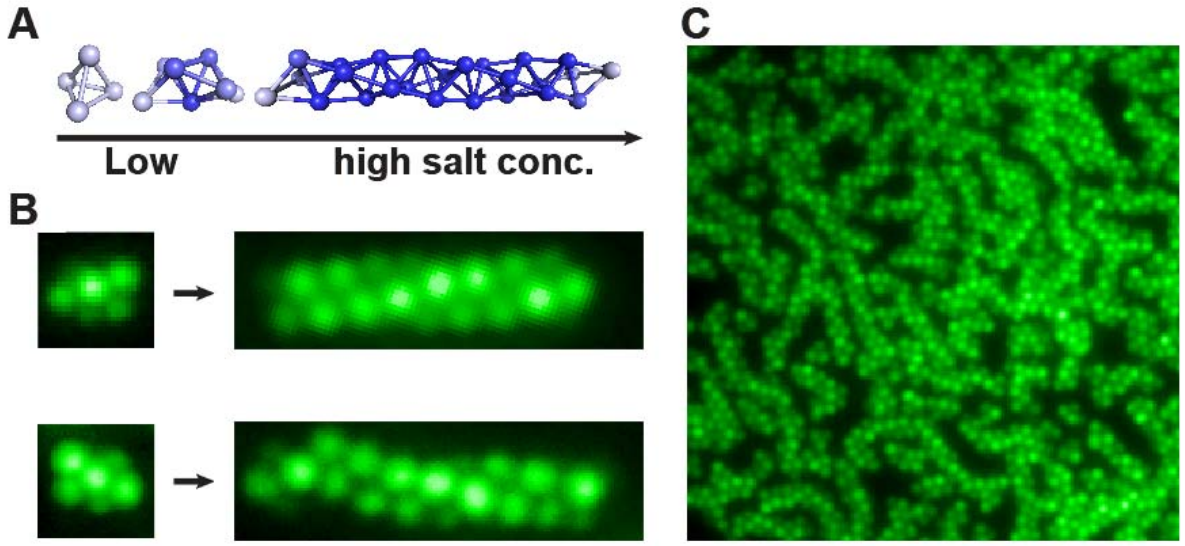

Fig. 3